Pathways of the Photocatalytic Reaction of Acetate in H2O and D2O Combined: An EPR and ATR-FTIR Study

Belhadj, H., Melchers, S., Robertson, P. K. J., & Bahnemann, D. W. (2016). Pathways of the Photocatalytic Reaction of Acetate in H2O and D2O Combined: An EPR and ATR-FTIR Study. Journal of Catalysis, 344, 831-840. DOI: 10.1016/j.jcat.2016.08.006

Published in:
Journal of Catalysis

Document Version:
Peer reviewed version

Pathways of the Photocatalytic Reaction of Acetate in H_2O and D_2O Combined: An EPR and ATR-FTIR Study

Hamza Belhadj[a,*], Stephanie Melchers[a], Peter K. J. Robertson[b] and Detlef W. Bahnemann[a,c,*]

[a]Institut für Technische Chemie, Leibniz Universität Hannover, Callinstraße 3, D-30167 Hannover, Germany.

[b]Centre for the Theory and Application of Catalysis (CenTACat), School of Chemistry and Chemical Engineering, Queen's University Belfast, Stranmillis Road, Belfast, BT9 5AG, UK.

[c]Laboratory ''Photoactive Nanocomposite Materials'', Saint-Petersburg State University, Ulyanovskaya str. 1, Peterhof, Saint-Petersburg, 198504 Russia.

Corresponding Author

*E-mail: belhadj@iftc.uni-hannover.de Telephone: +49-511-762-2773

*E-mail: bahnemann@iftc.uni-hannover.de Telephone: +49-511-762-5560

ABSTRACT

The adsorption and photocatalytic degradation of acetate on TiO_2 surfaces was investigated in H_2O and D_2O by ATR-FTIR and EPR Spectroscopy respectively. These studies were carried out in the dark and under UV(A) illumination to gain additional insights into the adsorption behaviour with the identification of paramagnetic species formed during the oxidation of acetate. Isotopic exchange during the adsorption of D_2O on TiO_2 surface led to different interactions between the adsorbate and OD groups. At different pH levels, several surface complexes of acetate can be formed such as monodentate, or bidentates. Under UV(A) irradiation of TiO_2 aqueous suspensions, the formation of hydroxyl and methoxy radicals evidenced as the corresponding spin-adducts, were found to dominate in alkaline and acidic suspensions respectively. Two possible pathways for the oxidation of acetate have been suggested at different pH levels in solution in terms of the source of the spin adduct formed. These proposed pathways were found to be in good agreement with ATR-FTIR and EPR results.

Keywords:

TiO_2, Acetate, Adsorption, D_2O, pH, Photocatalysis, *In-situ* ATR-FTIR, EPR spin trapping

INTRODUCTION

Titanium dioxide, (TiO_2), is an effective photocatalyst for the degradation of a broad range of organic pollutants [1]. The photocatalytic oxidation processes of organic pollutants is initiated by the formation of valence band holes (h^+_{vb}) and conduction band electrons (e^-_{cb}) which are formed in a TiO_2 particle upon ultra band gap illumination. Consequently, the TiO_2 particles act as electron donors and electron acceptors for molecules in the surrounding medium. For example, the holes may react with water and/or hydroxyl ions to form hydroxyl radicals, while

the excited electrons react with molecular oxygen to form superoxide radicals and hydrogen peroxide [2]. It was previously reported that the oxidation of organic pollutants on the surface of TiO_2 proceeds via two pathways [3]. One pathway involves photogenerated holes that oxidize adsorbed pollutant species directly. In the second pathway, pollutants are oxidized indirectly by free radicals produced at the TiO_2 surface.

Acetic acid/acetate has been used as the model pollutant by many research groups for the study of fundamental photocatalytic mechanisms. In oxygen free conditions, Muggli *et al*, reported that the photocatalytic decomposition of acetic acid on TiO_2 resulted in the formation of CO_2, with CH_4, and C_2H_6, as intermediate products [4],[5]. In aerated aqueous solution, Carraway *et al*, have shown that acetate is rapidly photooxidized on ZnO colloids to give formate and glyoxylate, as intermediate products which serve as effective electron donors on illuminated ZnO surfaces [6]. In another study, it was reported that during photocatalytic oxidation of acetic acid on platinized TiO_2, the methyl radical could be formed via two reaction pathways [4]. It was reported that in the presence of oxygen the photocatalytic degradation of acetate in a suspension of TiO_2 both the holes and hydroxyl radicals acted as oxidising species and it was suggested that two types of reactions may be responsible for the TiO_2 mediated photodegradation of acetate:[6]

(i) direct hole oxidation of adsorbed acetic acid/acetate molecules by photoinduced holes (h^+) at the valence band of TiO_2 semiconductor, or/and

(ii) indirect oxidation via hydroxyl radicals or other reactive oxygen species such as superoxide radicals and hydrogen peroxide.

In contrast, the adsorption of substrates were also one of the most important determinants for the photocatalytic degradation process. Robertson *et al.* suggested that the direct charge transfer to organic molecules required that the scavenging molecules were adsorbed on the TiO_2 surface prior to the adsorption of the photon [3]. Furthermore, the adsorption behaviour

of organic molecules were different during UV illumination [7]. Mendive *et al.* reported that the deaggregation of particles agglomerates occurred during UV irradiation resulting in an greater available surface area which in turn enhanced the photonic efficiency [8]. Adsorbed species such as water or molecular oxygen, together with the influence of pH are also expected to affect the degradation pathway on TiO_2 surface but their overall influences have yet to be clearly determined.

For a better understanding of the interfacial acetate/TiO_2 interactions, we have studied the adsorption of acetate on anatase surfaces (UV100) in H_2O and D_2O, as well as the formation of reactive oxygen species (ROS) using attenuated total reflection Fourier transform infrared (ATR-FTIR) and electron paramagnetic resonance (EPR) spectroscopy. This paper considers the effect of pH in terms of the adsorption behaviour of acetate on TiO_2 surfaces as well as the formation of primary intermediate radicals before and after UV(A) irradiation in order to provide further insight into the interfacial reaction mechanism of acetate decomposition during UV irradiation.

EXPERIMENTAL SECTION

Materials

TiO_2 (Hombikat UV100, 100% anatase) was kindly supplied by Sachtleben Chemie. Sodium acetate trihydrate (≥99.5%) was purchased from ROTH. The spin traps 5,5-dimethyl-1-pyrroline-N-oxide (DMPO) and Deuterium oxide (D_2O) (99.9 atom% D) were purchased from Sigma Aldrich. Deionized water (H_2O) was supplied from a Millipore Mill-Q system with a resistivity equal to 18.2 Ω cm at 25 °C. pH adjustments and measurements were performed using a Metrohm 691 model pH-meter using 0.5 mol L^{-1} of HNO_3 or NaOH.

ATR-FTIR Spectroscopic measurements

1- Preparation of TiO_2 film on the ATR-FTIR Crystal

Initially, an aqueous suspension of TiO_2 at a concentration of 5 g l^{-1} was prepared and sonicated for 15 min in an ultrasonic cleaning bath. An aliquot of 400 µL of the TiO_2 suspension was placed on the surface of the ZnSe ATR crystal and this small volume was simply spread by balancing the unit manually. The suspension was then dried by storing the crystal in a semi-opened desiccator at room temperature. Prior to deposition of the TiO_2 films, the ZnSe surfaces (area = 6.8 mm×72 mm) were cleaned by polishing with 1 mm diamond paste (Metadi II, polishing grade) and rinsed with methanol and deionised water. The coverage of the final dry layer of particles obtained was 2.3 g m^{-2} and the layer appeared to be very homogeneous under visual inspection. In the original preparation by Hug *et al*, Atomic Force Microscopy (AFM) measurements of layers with coverage of 2.3 g m^{-2} yielded a thickness of 1-3 µm.[9] The final resulting layers of particles remained stable over the entire course of the experiment. Thus, it was assumed that the effective path lengths at all wavelengths remained unchanged.

2- ATR FTIR measurement

The ATR-FTIR spectra of the TiO_2 samples were monitored by a FTIR spectrometer (IFS 66 BRUKER) equipped with an internal reflection element 45º ZnSe crystal and a deuterated triglycine sulfate (DTGS) detector. The interferometer and the infrared light path in the spectrometer were constantly purged with Argon and nitrogen to avoid H_2O and CO_2 contamination. The spectra were recorded with 300 scans at 4 cm^{-1} resolution and analyzed using OPUS version 6.5 software.

Irradiation of samples with UV(A) light were carried out using an LED lamp (Model LED-Driver, THORLABS) emitting UV light (365 nm). The distance from the UV lamp to the surface of the test solution was kept 30 cm on which the intensity of UV(A) light was of 1.0 $mWcm^{-2}$ as measured by UV radiometer (Dr. Honle GmbH, Martinsried, Germany).

In order to observe the interaction between water/deuterium oxide and acetate at TiO_2/aqueous solution interface, a first infrared spectrum was taken as a reference background. Prior to starting the irradiation experiments, spectra of adsorption of acetate (10^{-1} M) with H_2O or D_2O on the TiO_2 were monitored in the dark. When the last spectrum of each experiment had been recorded in the dark, the UV(A) lamp was turned on and another sequence of spectra was recorded.

EPR measurement

EPR spectra were recorded at room temperature on a MiniScope X-band EPR spectrometer (MS400 Magnettech GmbH, Germany) operating at 9.41 GHz field modulation. The acquisition parameters were as follows: centre field: 335.4086 mT, sweep time 60 s, number of points: 4096, number of scan: 1, modulation amplitude: 0.2 mT, power: 10 mW, gain: 5. The experimental EPR spectra acquisition and simulation was carried out using MiniScope and Winsim 2002 software.

The samples for EPR measurements were prepared as follows: TiO_2 (1g L^{-1}) was suspended in water or D_2O with concentration of acetate (10^{-3} M). The solution (10 ml) was stirred for at least 30 min in the dark to allow equilibration of the system. Before the measurement, 1 mL of 10^{-3} M acetate was introduced into the eppendorf tube and then 200 µL of 20 mM of DMPO was immediately added to the solution. The tube was shaken by hand to ensure homogenization of the sample. Subsequently, approximately 500 µL of this sample was immediately transferred into quartz flat cell cuvette (FZK 160-7×0.3) designed for EPR analysis. The samples were irradiated directly in the EPR spectrometer microwave cavity by a spot UV-light (LC8, Hamamatsu, 200 W super-quiet mercury-xenon lamp) through the quartz window of the cell for the experiments.

RESULTS

ATR-FTIR study

Adsorption of acetate in H_2O and D_2O on TiO_2

Fig. 1 and 2 show the time evolution of the spectra of adsorbed acetate on TiO_2 in H_2O (pH 6.0) and D_2O (pD 6.4) [10] respectively in the dark (a) and under UV(A) irradiation (b). The inserted figures show the time evolution of the ATR-FTIR spectral region at 2500-800 cm^{-1} (Fig.1) and 2000-800 cm^{-1} (Fig.2) where typical bands assigned to acetate anions can be clearly observed. The two most prominent peaks of the adsorbed acetate at 1450-1400 and 1600–1545 cm^{-1} are the symmetric and asymmetric stretching frequencies of the carboxylate ion (ν_{sy} COO and ν_{asy} COO) respectively [11]. Since the first infrared spectrum (water and acetate) was used as the background, a negative band of water bending mode was observed. The carbonyl zone was also observed from 1700 to 1500 cm^{-1}, and included C=O and O–C=O stretching modes [12]. However, these bands are obscured by relatively strong negative δ_{HOH} at 1638 cm^{-1} which are very similar to those obtained by other workers [13],[14]. The bands at 1045 cm^{-1} have previously been assigned in the literature to rocking CH_3 vibrations[15],[16] whereas the bands at 925-975 and 900 cm^{-1} can be assigned, respectively to C-C and OH bending [11],[17],[12]. On the other hand the adsorption of H_2O and D_2O take place on the TiO_2 surface which is represented by strong IR absorbance of the OH stretching (3000-3600 cm^{-1}) and OD stretching regions (2300-2700). In addition the bands at 1638 cm^{-1} and 1205 cm^{-1} can be assigned to the molecular bending modes of H_2O δ (H–O–H) and D_2O δ (D–O–D), respectively. It can be clearly seen from figure (Fig. 1a) that in the dark typical bands of adsorbed water as well as the band centred at 1045 cm^{-1}, which is assigned to the CH_3 group, have increased. A strong decrease in the intensities of carboxylate group, however, have also been detected. This negative band indicates the decrease in the IR intensity (I) with respect to I_0 due to the background subtraction [18],[14],[19]. The band observed at 2360 and 2342 cm^{-1} was assigned to the CO_2 group which decreased due to the desorption of molecular CO_2 contamination [8]. When D_2O was used instead of water, the shifting of D_2O band bending at 1205 cm^{-1} revealed

the same vibrational bands that corresponded to the symmetric and antisymmetric ν (COO^-) stretching vibrations (Fig. 2a). Furthermore, the intensity of the band of D_2O adsorption (OD stretching, D–O–D bending) also increased. Surprisingly, unlike the case of water adsorption, the intensity of the band assigned to CH_3 at 1045 cm^{-1} and OH bending at 900 cm^{-1} gradually decreased during the dark period. These results indicate that adsorption of D_2O on TiO_2 surfaces clearly affects the behaviour of acetate adsorption. Additionally, it is obvious from the spectra that the intensity of the OH-stretching band centred at 3269 cm^{-1} decreased gradually in the dark (Fig. 2a). Our previous study reported that in the dark the deuterated ion showed a stronger adsorption than hydroxyl ions on the surface of TiO_2, resulting in an isotopic exchange by replacing hydroxyl groups adsorbed on the TiO_2 surface (reaction 1) with OD groups [20].

$$\mathrm{Ti-OH} + \mathrm{OD^-} \longrightarrow \mathrm{Ti-OD} + \mathrm{OH^-} \qquad (1)$$

When the system was subsequently illuminated with UV(A) light in presence of oxygen, the intensity of the typical bands assigned to the acetate anions in H_2O (Fig. 1b) and D_2O (Fig. 2b) increased. The upward baseline shift following irradiation was interpreted as transient and persistent diffuse reflectance infrared signals due to the population of conduction band electrons upon irradiation of TiO_2 particles, where the baseline IR absorption for TiO_2 rises immediately upon UV irradiation [21],[14]. Meanwhile, the band at 1045 cm^{-1} assigned to the CH_3 rocking vibration increased and appeared to be stronger in water than in D_2O, with a shoulder at 972 cm^{-1} which could be assigned to the C-C band. Interestingly, although the interferometer was constantly purged with argon and nitrogen to avoid H_2O and CO_2 contamination, the intensity of the band assigned to CO_2 increased during UV(A) illumination. Furthermore in the region of OH stretching (Fig. 1b), an increase of the band at 3480 cm^{-1} was observed which could be assigned to the formation of H_2O_2 [20]. Conversely, as shown in figure 2b, the OH stretching band increased and shifted towards a higher wavenumber (3480

cm^{-1}) during UV(A) irradiation. These indicate the formation of these band can be attributed to photocatalytically generated CO_2 and H_2O_2 as photoproducts.

Effect of pH

Figure 3 and 4 show the evolution of the adsorbed acetate spectra in the dark a) and under UV(A) irradiation b) over time at pH 3 and 9 respectively. The pH values of the solution during UV (A) irradiation have been recorded (Table S1, Supplementary Information). In the IR spectrum, a similar adsorption behaviour with respect to the water band was observed in the dark. In contrast, the behaviour of acetate adsorption depended strongly on the solution pH. At pH 3 the band centred at 1066 cm^{-1} which includes the CH_3 vibration, showed a higher intensity compared to that observed at pH 9 where the band shifted and centred with a lower intensity at 964 cm^{-1} (Fig. 4a). The shifting of the absorption maximum with lower intensity can be explained by the interaction of the carboxylate ions with protons resulting in a small OH bending band at 900 cm^{-1}. The spectral development of acetate adsorption under UV illumination at pH 3 and 9 are shown in figures 3b and 4b, respectively. The symmetric and asymmetric stretching vibrations of carboxylate ions increased during UV irradiation. As can be seen clearly in the region of OH stretching the band at 3480 cm^{-1} assigned to Ti-OOH also increased during UV irradiation in acid and alkaline solutions. The behaviour of the CO_2 bands at 2360 and 2342 cm^{-1}, however, are clearly different. It is worth noting that at pH 6 (Fig. 1b) and pH 9 (Fig. 4b) the CO_2 band increased while at lower pH (Fig. 3b) the band decreased during UV(A) illumination. These results indicate that the photocatalytic reactions on the TiO_2 surfaces are different and depend strongly on solution pH.

EPR study

EPR spin-trapping studies of radicals generated

EPR spin-trap technique was employed using DMPO as a spin-trapping agent to probe the nature of the reactive oxygen species generated during the degradation of acetate in the

presence of molecular oxygen. Figure 5 shows the time course EPR spectra monitored by DMPO (spin-trap) at pH 6.0 in water (a) and pD 6.4 in D_2O (b) before and after UV(A) irradiation. As shown in figure 5, no EPR signals were observed in H_2O and D_2O when the reaction was performed in the dark. In contrast, under UV irradiation the photoexcitation of acetate (10^{-3}M) in TiO_2 aqueous suspensions in the presence of DMPO spin trap leads to the production of a four-line of EPR signal (with approximate intensities 1:2:2:1) in both H_2O and D_2O. The quartet peak intensity of the DMPO adduct with a 1:2:2:1 intensity in H_2O as well as in D_2O were virtually identical (Fig. 5b). The hyperfine parameters for the two DMPO adducts are: a_N= 1.477 mT, a_H= 1.485 mT, g= 2.0057; for the DMPO-OH adducts these are a_N= 1.477 mT, a_H= 1.485 mT, g= 2.0057. The DMPO-OH or DMPO-OD adducts are detailed in Figure S1, (Supplementary Information). To take into account the presence of isotopic exchange ($\mathrm{Ti-OH + OD^- \longrightarrow Ti-OD + OH^-}$) before UV(A) illumination, leads to the suggestion that these quartet peaks are assigned to a DMPO–OD adduct, which can be formed by oxidation of the D_2O or OD group [22]. It can be clearly observed, however, that after 1 min irradiation the intensity of the peaks gradually decreased.

Figure 6 shows the EPR spectra observed during the photocatalytic reaction at pH 9 (Fig. 6a) and pH 3 (Fig. 6b). As can be seen in the dark, such signals were not detected at either pH 9 or pH 3. When the sample was exposed to UV(A) irradiation at pH 9, however, four characteristic peaks of the DMPO-OH• adduct were observed with a maximum intensity after 3 min of irradiation which exhibits a hyperfine splitting constant a_N= 1.475 mT, a_H= 1.481 mT and g-value= 2.0057 (Figure S2, Supplementary Information). After that the EPR signal of DMPO-OH• completely decayed towards zero with continued UV irradiation (Fig. 6a). In contrast, at pH 3 (Fig. 6b), several peaks are formed. Due to spin-spin interactions these characteristic peaks might be assigned to a mixture of spin adducts of DMPO$-^{\bullet}OOH/O_2^{\bullet-}$ [23],[24] and DMPO-OCH_3 spin-adducts[25]. Brezova´ *et al* reported that the DMPO$-^{\bullet}OOH/O_2^{\bullet-}$ spin

adducts have very low stability and are converted to DMPO-OH• in aqueous media [26]. The simulation analysis of the experimental EPR spectra (Figure S3, Supplementary Information) revealed the interaction of EPR signals attributed to DMPO-OH (a_N= 1.475 mT, a_H= 1.475 mT; g= 2.0057) and DMPO-OCH_3 (a_N= 1.452 mT, a_H= 1.091 mT ; a_H^{γ} = 0.121 mT; g= 2.0057). The EPR spectrum corresponding to the DMPO-OH• are clearly observed. Therefore, the other-line EPR signal is most likely to be attributed to the DMPO-OCH_3 spin-adducts, which increased during the first 3 min of UV(A) irradiation. The hyperfine splitting constants of the methoxy radicals (DMPO-OCH_3) are similar to those reported by Zhu *et al.*[27] (Table S2, Supplementary Information). Furthermore, it was reported that methyl radicals may react immediately with molecular oxygen resulting in the generation of peroxomethyl radicals serving as a source of •DMPO–OCH_3 spin-adducts [26],[28]. Time dependent EPR spectra show that after 3 min of irradiation the signal intensity of the DMPO-OH and DMPO–OCH_3 adducts decrease during oxidation of acetate. These results clearly show the existence of different radical intermediates representing respectively, spin adducts of DMPO-OH• and DMPO-OCH_3 at pH 9 and pH 3, which would provide new insight into the mechanism of oxidation of acetate at different pH levels.

DISCUSSION

The photocatalytic activity for the decomposition of acetate depends strongly on two factors: the adsorption behaviour of acetate on TiO_2 surface and the effect of reactive oxygen species formed as part of the process. Therefore, it is important to elucidate the adsorption behaviour of acetate before and after UV(A) irradiation. As shown in figure 1 and 2, the spectrum of acetate adsorbed in the dark in H_2O and D_2O on TiO_2 is characterized by two strongly negative bands at 1450-1400 and 1600–1545 cm^{-1}, which can be assigned to symmetric ν_{sy} (COO^-) and asymmetric ν_{asy} (COO^-) stretching vibrations, respectively. It is important to consider,

however, that during the adsorption of acetate the adsorption of H_2O and D_2O yielded positive peaks (Fig. 1 and 2). Guan *et al.* remarked upon a competitive reaction between the adsorption of water and organic compounds, which was dominated by the water adsorption because of the surface acidity [29]. In the other hand, Rotzinger *et al* have reported that the adsorption of acetate on TiO_2 surface led to a specific reversible interaction of the carboxylate group with the TiO_2 surface [12]. Three different possibilities for the adsorption of carboxylate groups on TiO_2 surfaces have been proposed[12],[30],[31]: (i) As a bidentate structure, where both oxygen atoms bind to the same Ti atom. (ii) As monodentate replacing the basic OH group at the surface. (iii) As bidentate structure (bridging carboxylate) involving the carboxyl group and two Ti centres from the surface. The behaviour of acetate adsorption, however, is strongly influenced by the solution pH [30]. As can be seen clearly at pH 3 (Fig. 3a), the band centred at 1066 cm^{-1} which includes the CH_3 vibration increased in the dark compared to at pH 9 where the band shifted and centred with a lower intensity at 964 cm^{-1} (Fig. 4a). These results indicate that at pH < pH_{zpc} the interaction of TiO_2 with anions are favoured resulting in the formation of a bidentate structure involving two distinct Ti atoms (Scheme 1A). Recent theoretical work by Thornton *et al.*[32] has shown that the adsorption of acetic acid on anatase TiO_2 is more likely to be a bidentate structure. Nevertheless, as can be seen from the ATR-FTIR spectra in D_2O at neutral (pH ≈ pH_{zpc}), isotopic exchange (reaction 1) had a clear effect on the behaviour of adsorbed acetate, where the intensity of OH bending at 900 cm^{-1} decreased and ultimately disappeared in the dark (Fig. 2a). The disappearance of this band would suggest an interaction between the carboxylate and OD group resulting in a reduction of the amount of OH bending (Scheme S1, Supplementary Information). These results indicate that at pH values next to the pH_{zpc}, the acetate preferentially adsorbs on the positively charged anatase in the monodentate structure. This is facilitated by the presence of the hydrogen atom, which interacts with OH groups in the vicinity and these interactions are less intense due to the weakly charged surface

(Scheme 1B). Whereas at higher pH (Fig. 4a), the negative charged surface repulse the negative charged acetate anions resulting weak bonds such as hydrogen bonds or dipole-dipole interactions. (Scheme 1C).

Upon UV(A) irradiation an excited electron and positive hole are formed. The electron and hole may migrate to the catalyst surface where they can participate in redox reactions with adsorbed species. As can be seen from figure 1b and 2b, the typical bands of adsorbed acetate as well as the bands of H_2O and D_2O adsorption have increased during UV irradiation. Wang et al. revealed the fact that under UV(A) illumination the total exposed TiO_2 surface increases due to the de-aggregation of particles agglomerates which was explained by assuming that part of the absorbed light energy is converted non-adiabatically into heat which is subsequently used to break the bonds between the particles thus producing additional surface area for the photocatalytic process [7]. Recently, we have shown that the excitation of TiO_2 by UV light leads to an increase in the amount of adsorbed H_2O and D_2O in presence of oxygen by a photoinduced charge transfer process [20]. From this point of view the adsorption behaviour of acetate as well as the adsorption of intermediates formed during UV irradiation needs to be taken into account. This assumption was confirmed by increasing again the typical bands of adsorbed acetate during UV (A) illumination (Fig. 1b). As shown in Fig. 2b, unlike the case of water, at 900 cm^{-1} no increase of OH bending band have been detected in D_2O (Fig. 2b). This fact may interpreted as a new rearrangement of acetate adsorption resulting in the shift of OD band bending to lower frequency (< 800 cm-1). Thus, the formation of OH band bending was not possible anymore as schematically illustrated in Fig. 2b. Furthermore the intensity of the band of CH_3 formed at 1045 cm^{-1} is lower in D_2O compared in H_2O during UV irradiation. These results indicate a specific interaction of D_2O or /and OD group with intermediates on the TiO_2 surface during the degradation of acetate.

The effect of pH revealed the formation of the CO_2 bands at 2360 and 2342 cm^{-1} as well as the H_2O_2 band at 3480 cm^{-1} at pH > pH_{zpc}, (Fig. 1b and 4b), which can be considered as evidence for such adsorption intermediates being formed during oxidation of acetate. Interestingly, no formation of the CO_2 band was observed at pH 3 (Fig. 3b). From these results we suggest that the pathway for the degradation of acetate during UV irradiation is different and related to the pH of the solution. It was reported that the degradation rates of acetic acid depend strongly on the pH of the suspension. Carraway *et al*., reported that on acidic suspensions, formate and formaldehyde have been detected as the only products of the photocatalytic oxidation of acetate, while in alkaline suspensions, the main products are glycolate and formate accompanied by smaller amounts of glyoxylate and formaldehyde [6].

The EPR investigation showed that in alkaline suspensions, upon photoexcitation of TiO_2 in water, hydroxyl radicals are formed and this was confirmed by the addition of DMPO into the suspensions. This resulted in a significant increase of the DMPO–OH adduct EPR intensity (Fig. 6a). In contrast at lower pH levels, (pH 3) the signal intensity of hydroxyl radicals was negligible compared to that at pH 9 (Fig. 6b). These results suggest that at pH 9 the degradation of acetate mainly occurred by indirect oxidation via hydroxyl radical attack. Thus, the decrease of pH values of the solution only at pH 9 during UV(A) irradiation (Table1, Supplementary Information) indicate that in alkaline solution the hydroxyl radicals are being predominately formed by oxidation of hydroxyl ions in the water layer adsorbed on TiO_2 surfaces. On the other hand, Schuchmann *et al*, have reported that the hydroxyl radicals attack acetate ions primarily at the methyl group. The radicals that are subsequently formed react quickly with molecular oxygen leading to the formation of different products (Scheme 2A) [33],[34]. The existence of CO_2 and H_2O_2 as products was confirmed at pH 9 by means of *in situ* ATR-FTIR spectroscopy (Figure 4b). As can be seen clearly at pH 3, a new spin adduct of DMPO-OCH_3 has been also detected which was confirmed by Spin Fit simulations (Figure S3, Supplementary

Information). Figure 6b clearly shows that UV excitation of TiO_2 leads to an increase in the typical signal of methoxy radicals (DMPO-OCH_3; a_N= 1.452 mT, a_H= 1.091 mT; a_H^{γ} = 0.121 mT; g= 2.0057). This observation makes clear that the oxidation of acetate at pH 3 occurs mainly through direct oxidation by the hole (h^+) resulting in the well-known Kolbe decarboxylation with the formation of methyl radicals. Different products are then formed when these methyl radicals react with oxygen [26]. As expected at pH 3, no formation of CO_2 has been detected by ATR-FTIR spectroscopy (Fig. 3b), which confirms the validity of the proposed mechanism (Scheme 2B). In general, it is obvious from these results that the adsorption behaviour of acetate as well as the adsorption of water on TiO_2 surfaces play a vital role for the trapping of photogenerated charge carriers upon UV(A) irradiation, which is strongly dependent on the pH of the suspension.

CONCLUSION

As an *in-situ* technique, ATR- FTIR studies provide important evidence of the adsorption behaviour of acetate on TiO_2 surfaces before and after UV(A) irradiation. The experimental results have shown that the interaction of acetate with the TiO_2 surface depends strongly on the pH of the suspension. Under acidic pH conditions, the formation of a bidentate structure involving two distinct Ti atoms is favoured due to the interaction of TiO_2 with anions. At pH values next to the pH_{zpc}, the acetate preferentially adsorbs on the positively charged anatase in the monodentate structure. UV(A) irradiation of TiO_2 in the presence of molecular O_2 lead to the formation of H_2O_2 and CO_2 as photoproducts in alkaline solutions, whereas in acidic solution, the only product of H_2O_2 was detected. Results of the EPR study indicate that the degradation of acetate at pH 9 mainly occurred by indirect oxidation via hydroxyl radical attack whereas at pH 3 the degradation of acetate occurs via direct oxidation of surface-bound acetate by valence band holes.

ACKNOWLEDGEMENTS

Belhadj H. gratefully acknowledges a scholarship from the Deutscher Akademischer Austauschdienst (DAAD) providing the financial support to perform his Ph.D. studies in Germany. The present study was performed within the Project "Establishment of the Laboratory 'Photoactive Nanocomposite Materials'" No. 14.Z50.31.0016 supported by a Mega-grant of the Government of the Russian Federation.

Appendix A. Supplementary data

REFERENCES

[1] M.R. Hoffmann, S.T. Martin, W. Choi, D.W. Bahnemannt, Environmental Applications of Semiconductor Photocatalysis, Chem. Rev. 95 (1995) 69–96. doi:10.1021/cr00033a004.

[2] T. Hirakawa, Y. Nosaka, Properties of $O_2^{\bullet-}$ and $OH^{\bullet}$ Formed in TiO_2 aqueous suspensions by photocatalytic reaction and the influence of H_2O_2 and some ions, Langmuir. 18 (2002) 3247–3254. doi:10.1021/la015685a.

[3] P.K.J. Robertson, D.W. Bahnemann, J.M.C. Robertson, F. Wood, Photocatalytic Detoxification of Water and Air, in: Environ. Photochem. Part II, Springer-Verlag, Berlin/Heidelberg, 2005: pp. 367–423. doi:10.1007/b138189.

[4] D.S. Muggli, J.L. Falconer, Parallel Pathways for Photocatalytic Decomposition of Acetic Acid on TiO_2, J. Catal. 187 (1999) 230–237. doi:10.1006/jcat.1999.2594.

[5] D.S. Muggli, S. a Keyser, J.L. Falconer, Photocatalytic decomposition of acetic acid on TiO_2, Catal. Letters. 55 (1998) 129–132.

[6] E.R. Carraway, a J. Hoffman, M.R. Hoffmann, Photocatalytic oxidation of organic acids on quantum-sized semiconductor colloids., Environ. Sci. Technol. 28 (1994) 786–93. doi:10.1021/es00054a007.

[7] C. Wang, R. Pagel, J.K. Dohrmann, D.W. Bahnemann, Antenna mechanism and deaggregation concept: novel mechanistic principles for photocatalysis, Comptes Rendus Chim. 9 (2006) 761–773. doi:10.1016/j.crci.2005.02.053.

[8] C.B. Mendive, D. Hansmann, T. Bredow, D. Bahnemann, New insights into the mechanism of TiO_2 photocatalysis: Thermal processes beyond the electron-hole creation, J. Phys. Chem. C. 115 (2011) 19676–19685. doi:10.1021/jp112243q.

[9] S.J. Hug, B. Sulzberger, In situ Fourier Transform Infrared Spectroscopic Evidence for

the Formation of Several Different Surface Complexes of Oxalate on TiO_2 in the Aqueous Phase, Langmuir. 10 (1994) 3587–3597. doi:10.1021/la00022a036.

[10] A. Krężel, W. Bal, A formula for correlating pKa values determined in D_2O and H_2O, J. Inorg. Biochem. 98 (2004) 161–166. doi:10.1016/j.jinorgbio.2003.10.001.

[11] J.-J. Max, C. Chapados, Infrared Spectroscopy of Aqueous Carboxylic Acids: Comparison between Different Acids and Their Salts, J. Phys. Chem. A. 108 (2004) 3324–3337. doi:10.1021/jp036401t.

[12] F.P. Rotzinger, J.M. Kesselman-Truttmann, S.J. Hug, V. Shklover, M. Grätzel, Structure and Vibrational Spectrum of Formate and Acetate Adsorbed from Aqueous Solution onto the TiO_2 Rutile (110) Surface, J. Phys. Chem. B. 108 (2004) 5004–5017. doi:10.1021/jp0360974.

[13] F. Guzman, S.S.C. Chuang, Tracing the reaction steps involving oxygen and IR observable species in ethanol photocatalytic oxidation on TiO_2, J. Am. Chem. Soc. 132 (2010) 1502–1503. doi:10.1021/ja907256x.

[14] D. Gong, V.P. Subramaniam, J.G. Highfield, Y. Tang, Y. Lai, Z. Chen, In situ mechanistic investigation at the liquid/solid interface by attenuated total reflectance FTIR: Ethanol photo-oxidation over pristine and platinized TiO_2 (P25), ACS Catal. 1 (2011) 864–871. doi:10.1021/cs200063q.

[15] L.H. Jones, Infrared Spectra and Structure of the Crystalline Sodium Acetate Complexes of U(VI), Np(VI), Pu(VI), and Am(VI). A Comparison of Metal-Oxygen Bond Distance and Bond Force Constant in this Series, J. Chem. Phys. 23 (1955) 2105. doi:10.1063/1.1740675.

[16] K. Ito, H.J. Bernstein, the Vibrational Spectra of the Formate, Acetate, and Oxalate Ions, Can. J. Chem. 34 (1956) 170–178. doi:10.1139/v56-021.

[17] J. Coates, Interpretation of Infrared Spectra, A Practical Approach, Encycl. Anal. Chem. (2000) 10815–10837. doi:10.1002/9780470027318.

[18] A.R. Almeida, J. a. Moulijn, G. Mul, In situ ATR-FTIR study on the selective photo-oxidation of cyclohexane over anatase TiO_2, J. Phys. Chem. C. 112 (2008) 1552–1561. doi:10.1021/jp077143t.

[19] J.M. Kesselman-Truttmann, S.J. Hug, Photodegradation of 4,4 ’-bis(2-sulfostyryl)biphenyl (DSBP) on metal glides followed by in situ ATR-FTIR spectroscopy, Environ. Sci. Technol. 33 (1999) 3171–3176. doi: 10.1021/es981226t

[20] H. Belhadj, A. Hakki, P.K.J. Robertson, D.W. Bahnemann, In situ ATR-FTIR study of H_2O and D_2O adsorption on TiO_2 under UV irradiation, Phys. Chem. Chem. Phys. 17 (2015) 22940–22946. doi:10.1039/C5CP03947A.

[21] S.H. Szczepankiewicz, a J. Colussi, M.R. Hoffmann, Infrared Spectra of Photoinduced Species on Hydroxylated Titania Surfaces, J. Phys. Chem. B. 104 (2000) 9842–9850. doi:10.1021/jp0007890.

[22] K. Makino, T. Hagiwara, A. Murakami, A mini review: Fundamental aspects of spin trapping with DMPO, Int. J. Radiat. Appl. Instrumentation. Part. 37 (1991) 657–665. doi:10.1016/1359-0197(91)90164-W.

[23] H. Fu, L. Zhang, S. Zhang, Y. Zhu, J. Zhao, Electron spin resonance spin-trapping detection of radical intermediates in N-doped TiO2-assisted photodegradation of 4-

chlorophenol., J. Phys. Chem. B. 110 (2006) 3061–5. doi:10.1021/jp055279q.

[24] M. Polovka, EPR spectroscopy: A tool to characterize stability and antioxidant properties of foods, J. Food Nutr. Res. 45 (2006) 1–11.

[25] D. Dvoranová, Z. Barbieriková, V. Brezová, Radical Intermediates in Photoinduced Reactions on TiO_2 (An EPR Spin Trapping Study), Molecules. 19 (2014) 17279–17304. doi:10.3390/molecules191117279.

[26] V. Brezová, S. Gabčová, D. Dvoranová, A. Staško, Reactive oxygen species produced upon photoexcitation of sunscreens containing titanium dioxide (an EPR study), J. Photochem. Photobiol. B Biol. 79 (2005) 121–134. doi:10.1016/j.jphotobiol.2004.12.006.

[27] B.-Z. Zhu, H.-T. Zhao, B. Kalyanaraman, J. Liu, G.-Q. Shan, Y.-G. Du, B. Frei, Mechanism of metal-independent decomposition of organic hydroperoxides and formation of alkoxyl radicals by halogenated quinones, Proc. Natl. Acad. Sci. 104 (2007) 3698–3702. doi:10.1073/pnas.0605527104.

[28] A. Marchaj, D.G. Kelley, A.B. Bakac, J.H. Espenson, Kinetics of the Reactions Between Alkyl Radicals and Molecular Oxygen in Aqueous Solution, J. Phys. Chem. 95 (1991) 4440–4441.

[29] K. Guan, Relationship between photocatalytic activity, hydrophilicity and self-cleaning effect of TiO_2/SiO_2 films, Surf. Coatings Technol. 191 (2005) 155–160. doi:10.1016/j.surfcoat.2004.02.022.

[30] S.J. Hug, D. Bahnemann, Infrared spectra of oxalate, malonate and succinate adsorbed on the aqueous surface of rutile, anatase and lepidocrocite measured with in situ ATR-FTIR, J. Electron Spectros. Relat. Phenomena. 150 (2006) 208–219. doi:10.1016/j.elspec.2005.05.006.

[31] M.F. Atitar, H. Belhadj, R. Dillert, D.W. Bahnem, The Relevance of ATR-FTIR Spectroscopy in Semiconductor Photocatalysis, in: Emerg. Pollut. Environ. - Curr. Furth. Implic., InTech, 2015. doi:10.5772/60887.

[32] D.C. Grinter, M. Nicotra, G. Thornton, Acetic Acid Adsorption on Anatase TiO_2 (101), J. Phys. Chem. C. 116 (2012) 11643–11651. doi:10.1021/jp303514g.

[33] H.Z. and C. von S. Man Nien Schuchmann, Acetate Peroxyl Radicals, 0_2CH_2C0: A Study on the y-Radiolysis and Pulse Radiolysis of Acetate in Oxygenated Aqueous Solutions, Zeitschrift Für Naturforsch. 40b (1985) 1015–1022. http://inis.iaea.org/search/search.aspx?orig_q=RN:17081730.

[34] H.-P. Schuchmann, C. von Sonntag, Methylperoxyl radicals: a study of the γ-radiolysis of methane in oxygenated aqueous solutions, Zeitschrift Für Natürforsch. 39b (1984) 217–221. doi:10.1515/znb-1984-0217.

Figure captions

Figure 1: Time evolution of the ATR–FTIR spectra of adsorbed acetate in the presence of O_2 on TiO_2 at pH 6.0 a) in the dark for 3 h, b) under 6 h of UV(A) illumination.

Figure 2: Time evolution of the ATR–FTIR spectra of adsorbed acetate in D_2O in the presence of O_2 on TiO_2 at pD 6.4 a) in the dark for 3 h, b) under 6 h of UV(A) illumination.

Figure 3: Time evolution of the ATR–FTIR spectra of adsorbed acetate in the presence of O_2 on TiO_2 at pH 3, a) in the dark for 3 h, b) under 6 h of UV(A) illumination.

Figure 4: Time evolution of the ATR–FTIR spectra of adsorbed acetate in the presence of O_2 on TiO_2 at pH 9, a) in the dark for 3 h, b) under 6 h of UV(A) illumination.

Figure 5. DMPO spin-trapping EPR spectra in the dark and under UV(A) irradiation at pH 6.0 in water (a) DMPO-OH (a_N = 1.477 mT, a_H = 1.485 mT; g = 2.0057) and pD 6.4 in D_2O (b) DMPO-OD (aN = 1.477 mT, aH = 1.485 mT; g = 2.0057)

Figure 6. DMPO spin-trapping EPR spectra in the dark and under UV(A) irradiation at pH 9 (a) DMPO-OH (aN = 1.475 mT, aH = 1.481 mT; g = 2.0057) and pH 3 (b) DMPO–OH adducts (aN = 1.475 mT, aH = 1.475 mT; g = 2.0057) and DMPO-OCH_3 adducts (a_N= 1.452 mT, a_H= 1.091 mT ; a_H^{γ} = 0.121 mT; g = 2.0057).

Scheme 1 Schematic representation for the adsorption of acetate on anatase surface (UV100) in the dark at pH < pH_{zpc} (A), pH ≈ pH_{zpc} (B), pH > pH_{zpc} (C).

Scheme 2 Proposed mechanism for the photocatalytic reaction of acetate at pH 9 (A) and pH 3 (B)

Graphical abstract

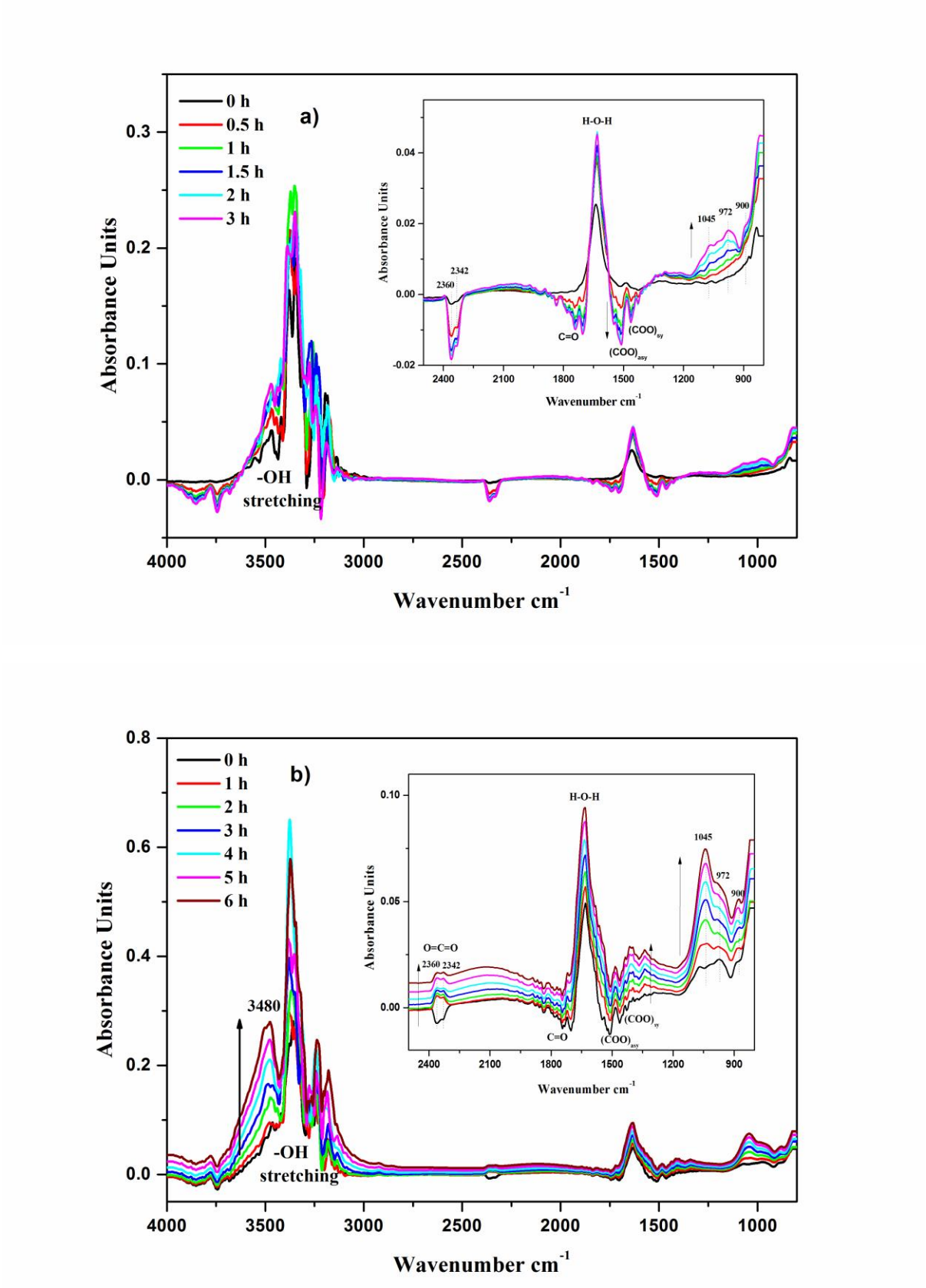

Figure 1: Time evolution of the ATR–FTIR spectra of adsorbed acetate in the presence of O_2 on TiO_2 at pH 6.0 a) in the dark for 3 h, b) under 6 h of UV(A) illumination.

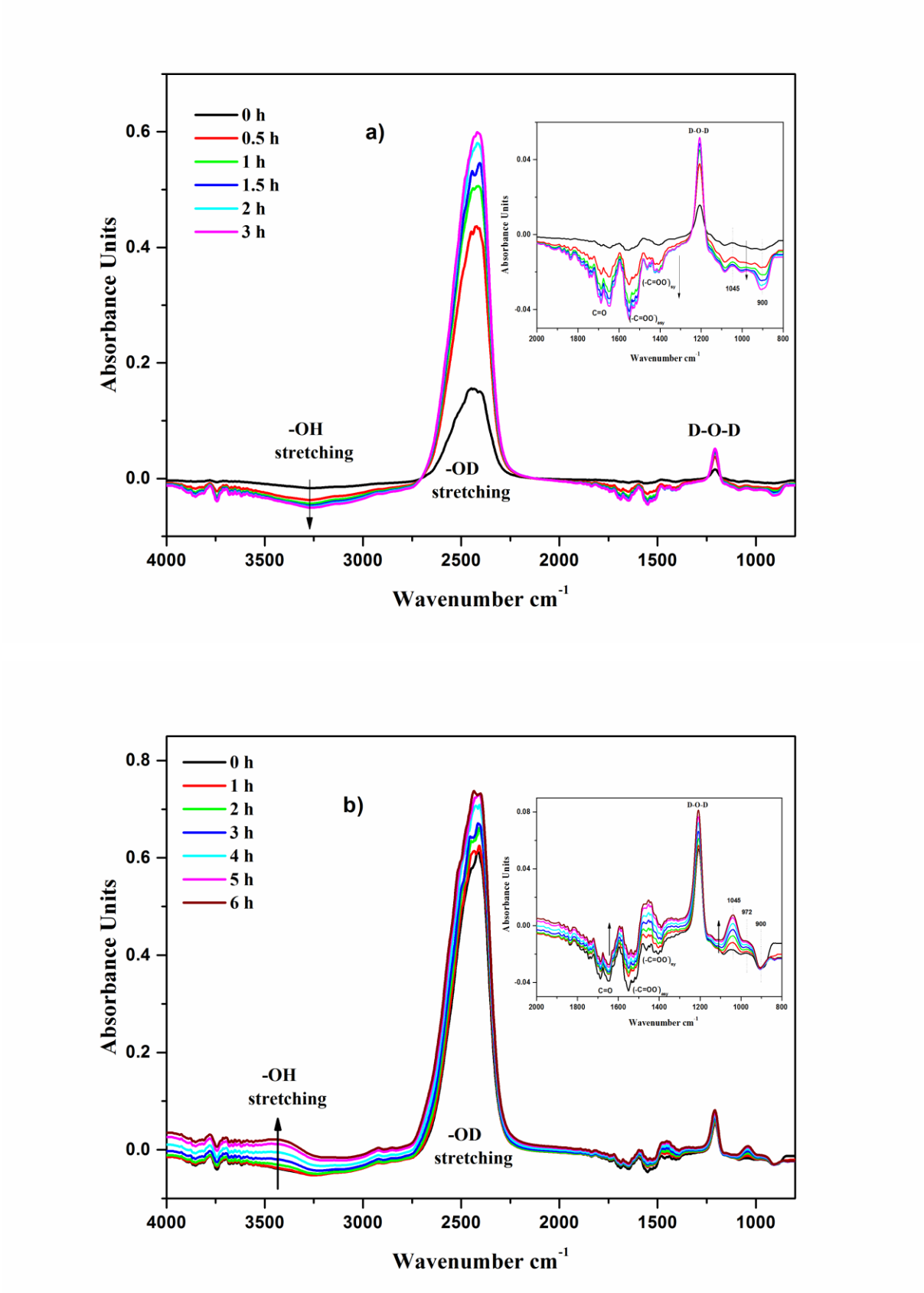

Figure 2: Time evolution of the ATR–FTIR spectra of adsorbed acetate in D_2O in the presence of O_2 on TiO_2 at pD 6.4 a) in the dark for 3 h, b) under 6 h of UV(A) illumination.

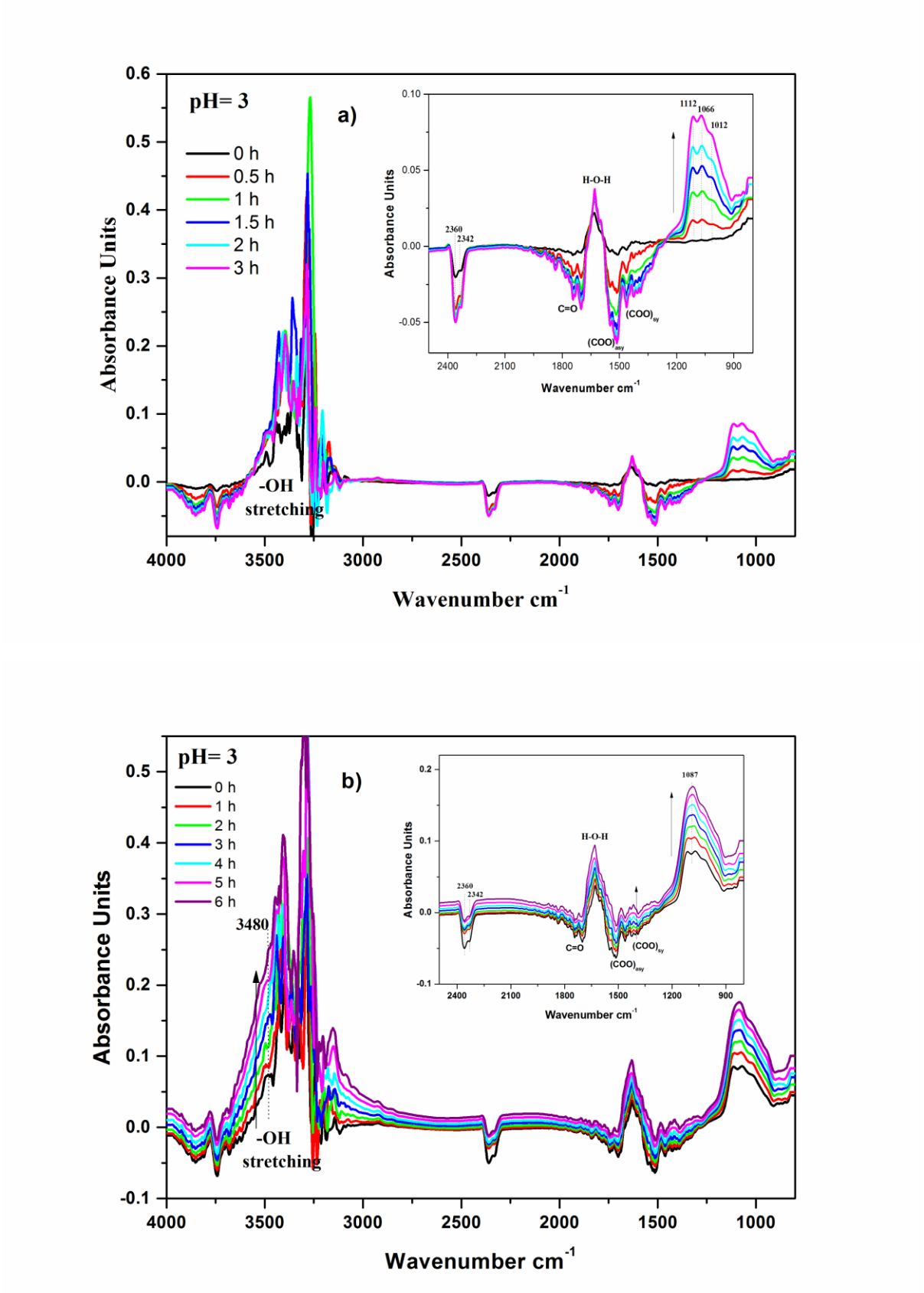

Figure 3: Time evolution of the ATR–FTIR spectra of adsorbed acetate in the presence of O_2 on TiO_2 at pH 3, a) in the dark for 3 h, b) under 6 h of UV(A) illumination.

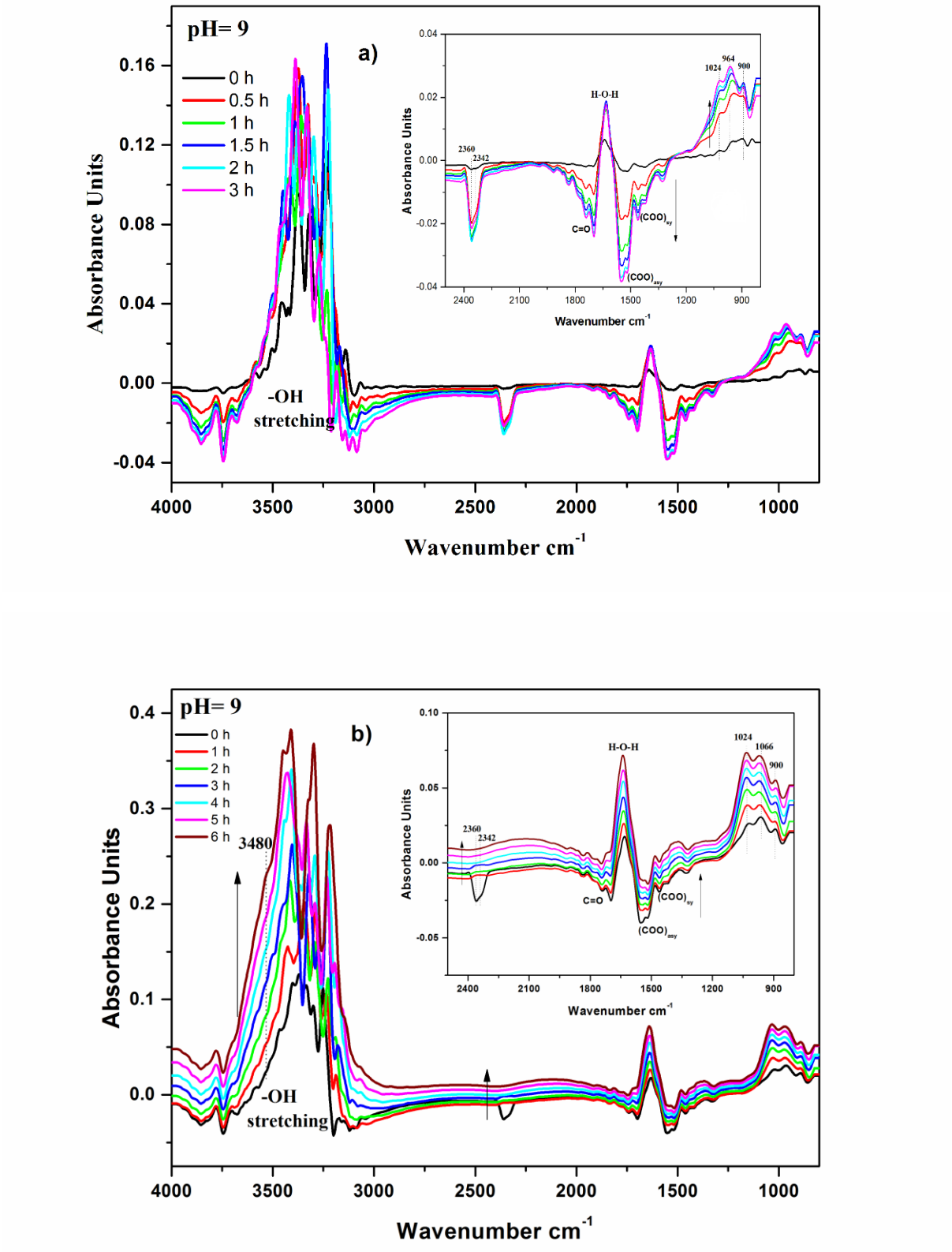

Figure 4: Time evolution of the ATR–FTIR spectra of adsorbed acetate in the presence of O_2 on TiO_2 at pH 9, a) in the dark for 3 h, b) under 6 h of UV(A) illumination.

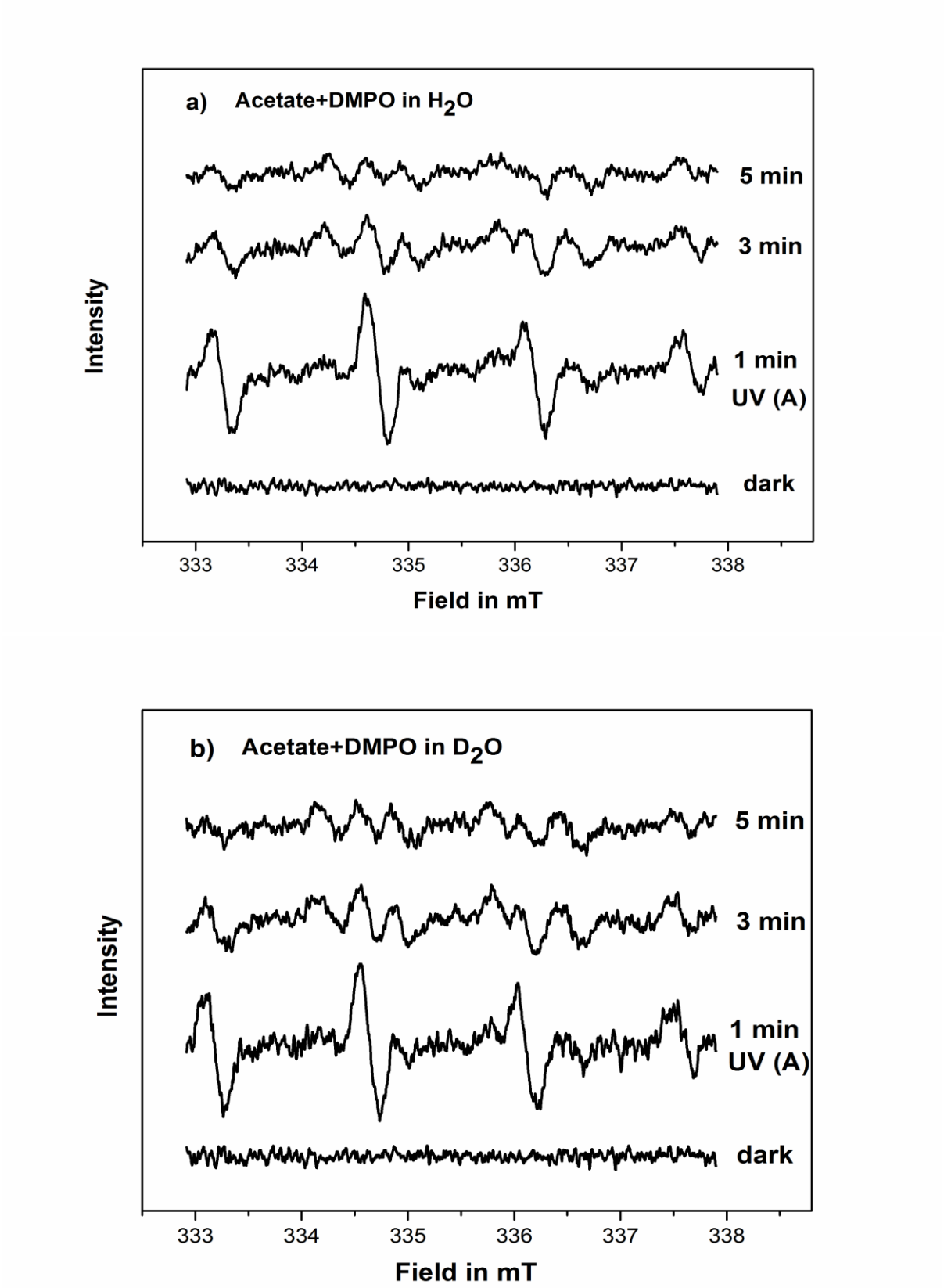

Figure 5. DMPO spin-trapping EPR spectra in the dark and under UV(A) irradiation at pH 6.0 in water (a) DMPO-OH (a_N = 1.477 mT, a_H = 1.485 mT; g = 2.0057) and pD 6.4 in D_2O (b) DMPO-OD (a_N = 1.477 mT, a_H = 1.485 mT; g = 2.0057)

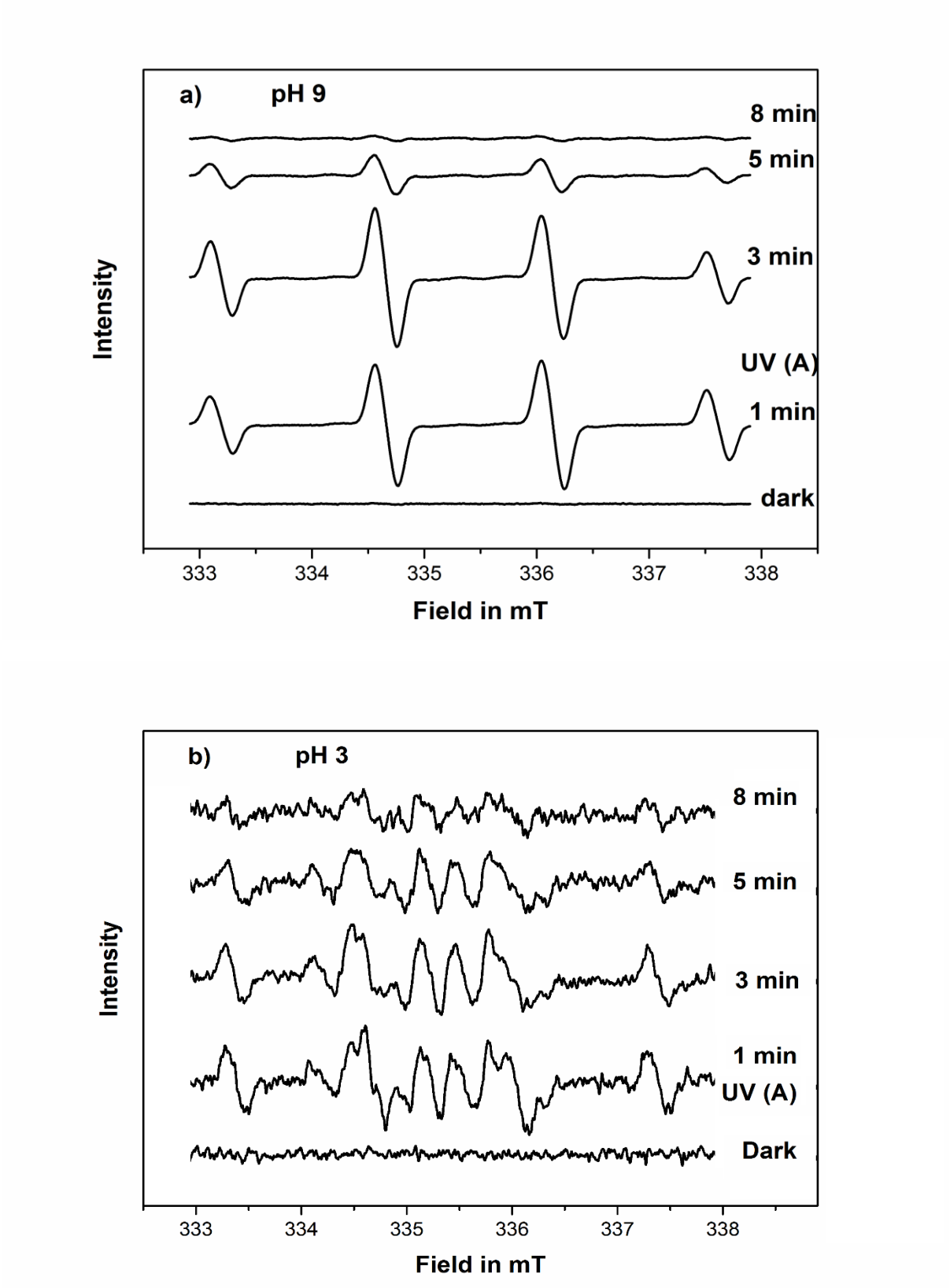

Figure 6. DMPO spin-trapping EPR spectra in the dark and under UV(A) irradiation at pH 9 (a) DMPO-OH (a_N = 1.475 mT, a_H = 1.481 mT; g = 2.0057) and pH 3 (b) DMPO–OH adducts (a_N = 1.475 mT, a_H = 1.475 mT; g = 2.0057) and DMPO-OCH_3 adducts (a_N= 1.452 mT, a_H= 1.091 mT ; a_H^{γ} = 0.121 mT; g = 2.0057).

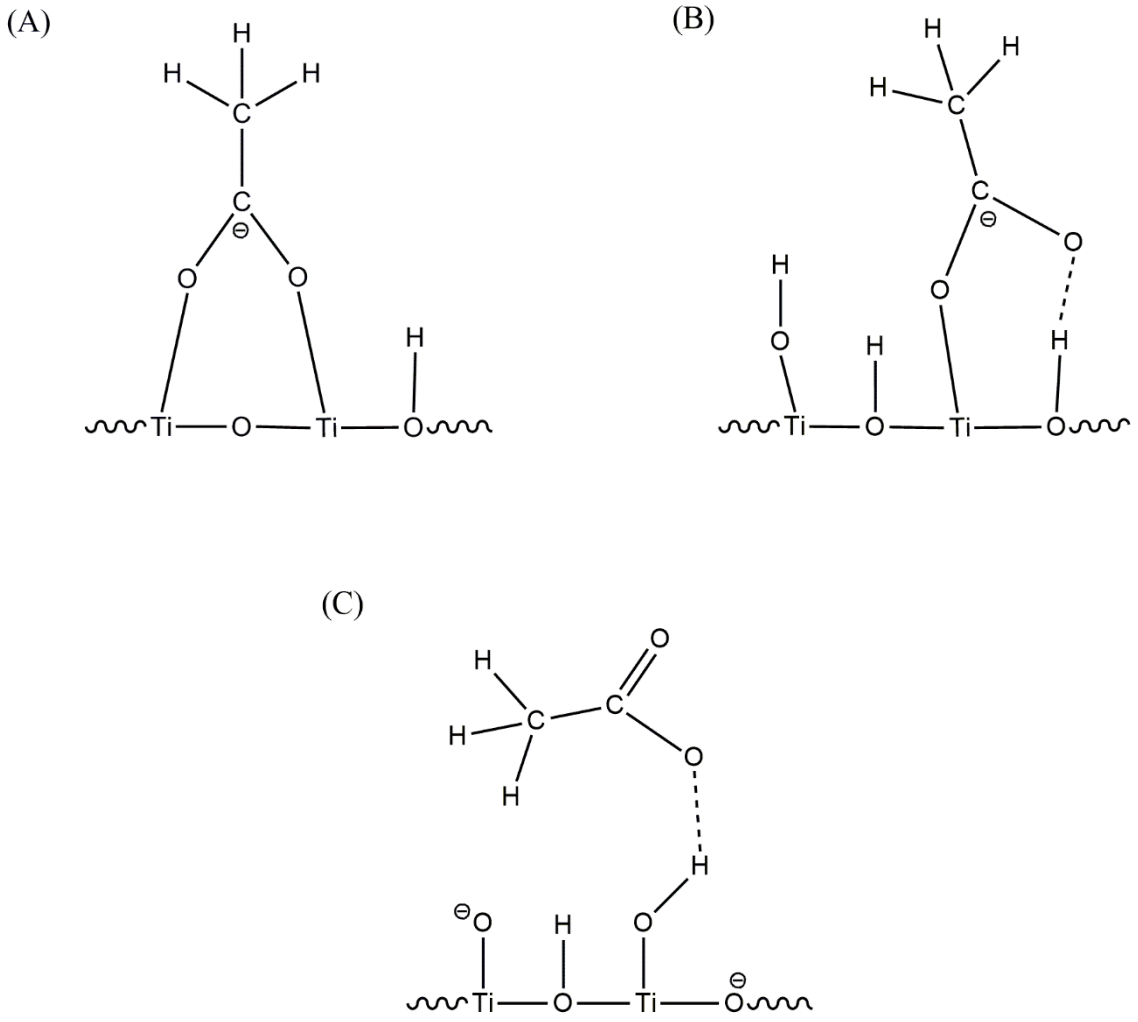

Scheme 1 Schematic representation for the adsorption of acetate on anatase surface (UV100) in the dark at pH < pH_{zpc} (A), pH ≈ pH_{zpc} (B), pH > pH_{zpc} (C).

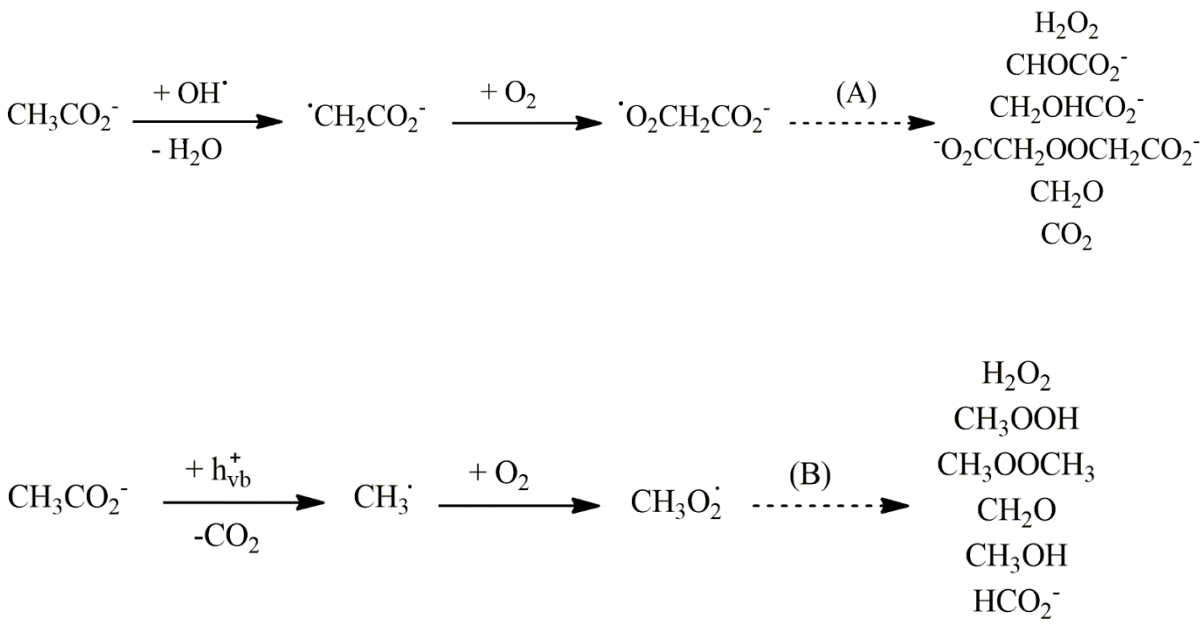

Scheme 2 Proposed mechanism for the photocatalytic reaction of acetate at pH 9 (A) and pH 3 (B)

Graphical abstract